A Method to Estimate the Ionospheric bias by Using the New GNSS Frequencies: An Analysis of its Theoretical Accuracy in a PPP Context

M. C. DE LACY[1], A. J. GIL[1], G. RODRÍGUEZ-CADEROT[2] and B. MORENO[2]

[1] Dept. Ingeniería Cartográfica, Geodésica y Fotogrametría - Universidad de Jaén, Spain
(mclacy@ujaen.es; ajgil@ujaen.es)

[2] Sec. Dptal. Astronomía y Geodesia. Universidad Complutense de Madrid, Spain
(grc@mat.ucm.es; bmorenom@mat.ucm.es)

(Received 25 February 2008; received in revised form, 13 March 2008; accepted 18 April 2008)

ABSTRACT
The modernization of the Global Positioning System (GPS) and the advent of the European Project Galileo will lead to a multifrequency Global Navigation Satellite System (GNSS). Single GNSS receiver observations could be used to estimate the ionospheric bias and smoothed pseudoranges which, in turn, can be exploited to better estimate the absolute position of the receiver and its clock correction. In fact, if we consider the satellite ephemerides and satellite clock corrections as perfect quantities (i. e. not affected by errors), the adjustment of GNSS observations is broken down into two parts. In addition, the least squares (LS) theory leads to a feasible adjustment in two steps, where covariance matrices can be explicitly written, studied and propagated from one step to the other, so that, a rigorous solution is finally obtained. This paper deals with the analytic representation of the above mentioned LS procedure and provides theoretical limits for the achievable accuracies of the parameter estimated considering different scenarios, including modernized GPS and Galileo systems. Furthermore, numerical tests with Galileo data simulated by GSSF (Galileo System Simulation Facility) have been carried out.
Key words: Modernized GPS, Galileo, ionospheric bias, formal accuracy.

RESUMEN
La modernización del Sistema de Posicionamiento Global (GPS) y la llegada del Proyecto Europeo Galileo, darán lugar a un Sistema de Navegación por Satélite (GNSS) multifrecuencia. Las observaciones de un único receptor GNSS podrán emplearse en la estimación del efecto ionosférico y las pseudodistancias suavizadas, las cuales, a su vez, se utilizarán en la estimación de la posición absoluta del receptor y la corrección del reloj. Considerando las efemérides de los satélites y las correcciones a los relojes de los satélites como cantidades perfectas (i. e. no afectadas de errores), el ajuste de observaciones GNSS se divide en dos partes. La teoría mínimo cuadrática proporciona un ajuste en dos etapas en el cual, las matrices de covarianza pueden escribirse explícitamente y propagarse de un paso al siguiente, de forma que, finalmente obtenemos una solución rigurosa. En este trabajo se muestra la representación analítica del procedimiento mínimos cuadrados mencionado anteriormente y se proporcionan límites teóricos para las precisiones alcanzables en la estimación de los parámetros al conside-

rar diferentes escenarios, incluyendo los sistemas GPS modernizado y Galileo. Adicionalmente, se han llevado a cabo test numéricos con datos Galileo simulados con el simulador GSSF (Galileo System Simulation Facility).
Palabras clave: GPS Modernizado, Galileo, efecto Ionosférico, precisión teórica.

1. INTRODUCTION

The GNSS observables depend on the satellite-receiver distance, atmospheric effects, satellite and receiver offsets and phase ambiguities, as well as satellite and receiver equipment delays. GNSS observations can be used to estimate the ionsopheric bias and the user position. The main obstacle in the estimation of the ionospheric TEC (Total Electron Content) from dual frequency GPS data is the effect of the pseudorange electronic biases, while the carrier phase equipment delays are absorbed by the ambiguity parameters. A pseudorange bias is present for each of the two GPS frequencies, and the difference between them is called differential code bias (DCB). Several authors have studied the problem of estimating the TEC and the differential code biases. Coco et al. (1991) represented the vertical TEC using polynomial coefficients. Three years later, (Sardon et al. 1994) used a Kalman filtering approach to estimate the TEC and the DCBs. At the end of 1996, CODE (Center for Orbit Determination in Europe) began to produce daily global ionosphere maps (GIMs) using a spherical harmonic expansion to represent the TEC (http://www.aiub.unibe.ch/ionosphere). In 1999, (Schaer, 1999) studied the time series of the coefficients of the expansion into spherical harmonics used to represent the TEC. (Lacy et al., 2005) presented a procedure based on the LS approach, which implicitly takes into account these equipment biases in the estimation of the ionospheric effect. Another method is shown in (Portillo et al., 2008). In this paper, a Precise Point Positioning (PPP) approach based on undifferenced multifrequency GPS observations and LS theory is presented. This procedure will allow us to estimate the position of the station and the inospheric bias by exploiting the presence of new frequencies in the future GNSS context, and furthermore, analyze the formal accuracy of the different parameters estimated. In particular, in Section 2, the GNSS observation equations in a multifrequency scenario are described; in Section 3, our method is introduced. In Section 4, the numerical tests regarding the limits of achievable formal accuracies are shown. Finally, results coming from simulated data by GSSF are studied.

2. THE FUTURE GNSS SCENARIO

The modernization of the GPS and the advent of the Galileo system will lead to a multifrequency GNSS system improving the capability of the precise positioning applications. Details of the satellite constellation and frequencies for modernized GPS and future Galileo can be found in (Simsky et al, 2006). Table 1 summarizes the GPS and Galileo signals frequencies.

Table 1.- Basic GPS (L) and Galileo (E) signal frequencies.

Carrier	Frecuency (MHz)
L1	1575.42
L2	1227.6
L5	1176.45
E2-L1-E1	1575.42
E5b	1207.14
E5a	1176.14

In 1991, Euler and Goad (1991) assumed some approximations in a general model of GPS observables in order to express them in a more suitable form. Taking these simplifications into account and omitting the indices related to receiver and satellite, the mathematical model of GNSS carrier phase and pseudorange observables specific to a receiver and a satellite (i.e., for undifferenced data) for an epoch is the following:

$$\begin{cases} P_k(t) = \rho(t) + K_{1k}\, J_1(t) + v_P(t) \\ L_k(t) = \rho(t) - K_{1k}\, J_1(t) + B_k + v_L(t) \end{cases} \quad (1)$$

Where $k = 1, 2, 3$, f_k being the frequencies shown in Table 1. The symbols P_k and L_k are the code pseudorange measurements and the carrier phase observations expressed in distance units at frequency f_k, respectively; $K_{1k} = \left(f_1/f_k\right)^2$; v_P and v_L represent the measurement noise of code pseudoranges and phase obvservations, respectively. All parameters in the above equations are generally biased. The term is interpreted as the distance travelled by the signal and is biased by clock terms and tropospheric delay effect. J_1 is the ionospheric group delay at the f_1 frequency. The term B_k is formed by joining the non-zero initial phase and the integer carrier phase ambiguity. That is to say that the initial carrier phase ambiguity at frequency f_k is biased by initialization constants and generally is not integer. Furthermore, each of the equations in (1) is known to be biased by a term known as equipment delay, which is constant for a short period of time and represents the travel time of the signal through the circuitries of the receiver and satellite. The multipath effect is ignored in equations (1).

The presence of new frequencies will imply that many different frequency combinations will be able to be generated. If we consider phase observations expressed as cycle units, a general linear combination (LC) of phase observations in a triple frequency scenario can be written as

$$\Phi_{LC} = m_1\Phi_1 + m_2\Phi_2 + m_3\Phi_3 \quad (2)$$

Table 2.- GPS and Galileo widelane linear combinations

System	LC	m_1	m_2	m_3	Wavelength (m)
GPS	EWL	0	1	–1	5.81
	WL	1	–1	0	0.862
	ML	1	0	–1	0.751
Galileo	EWL	0	1	–1	9.768
	WL	1	–1	0	0.814
	ML	1	0	–1	0.751

where Φ_k with k = 1, 2, 3 represent phase observations (in cycles) at the frequency f_k. The coefficients of the corresponding linear combination and their wavelengths are shown in Table 2. In this table, EWL, WL and ML stand for extrawidelane, widelane and mediumlane combination (Zhang, 2005). These linear combinations represent the generalization of the traditional widelane combination of dual frequency GPS phase observations.

3. A METHOD FOR THE POSITION AND IONOSPHERIC BIAS ESTIMATION

In our method, the LS theory is used twice in order to obtain the receiver position. In a first step, the LS theory is used to estimate smoothed pseudoranges, ionospheric effect, and ambiguity parameters. In the second one, the LS theory is applied to estimate the receiver clock offset and the station position.

In the near future, GNSS triple frequency receivers will be available. In this case, the mathematical model of GNSS code and phase observations can be written as:

$$\begin{cases} \underline{P}\,(t) = A_1 \underline{\zeta}\,(t) + \underline{v}_P\,(t) \\ \underline{L}\,(t) = A_2 \underline{\zeta}\,(t) + \underline{B} + \underline{v}_L\,(t) \end{cases} \tag{3}$$

Where $\underline{\zeta}\,(t)$ is a vector representing the smoothed pseudorange (satellite-receiver pseudorange obtained by combining code and phase observation) and ionospheric delay at each epoch t; $\underline{B}$ is the vector of ambiguity biases and $\underline{v}_P$, $\underline{v}_L$ are the measurement errors.

The observation vector at any epoch t is given by:

$$\underline{y}_0\,(t) = \left(\underline{P}(t), \underline{L}\,(t)\right)^+ = \left(P_1(t), P_2(t), P_3(t), L_1(t), L_2(t), L_3(t)\right)^+ \tag{4}$$

The stochastic model at any epoch t is:

$$C = \sigma_0^2 \begin{pmatrix} Q_P & 0 \\ 0 & I_3 \end{pmatrix} \tag{5}$$

Where Q_P is the cofactor matrix relative to the code measurements at any given epoch t, I_3 is the 3 x 3 identity matrix and σ_0^2 represents the a priori variance. By hypothesis, we will consider that the a priori covariance matrix of the observations is diagonal, and the standard deviations for the carrier phase and pseudorange observations are in the order of millimeters and decimeters, respectively. In spite of this hypothesis, it is important to remember that some receivers filter the observations in order to reduce the measurement noise; this procedure cause correlations between the observables (Bona, 2000).

The unknown parameters are:

1. Ambiguity biases at first, second and third frequency. We will assume absence of cycle slips. Then, ambiguity biases should be constant over our observation period. The LS estimate of these parameters will be denoted as $\hat{\underline{B}}$.
2. Smoothed pseudoranges and ionospheric delays at each epoch t with $t = t_1, t_2, \ldots, t_n$.

The design matrix A is given by:

$$A = \begin{pmatrix} A_1 & 0 & 0 & \ldots & 0 \\ A_2 & 0 & 0 & \ldots & I_3 \\ 0 & A_1 & 0 & \ldots & 0 \\ 0 & A_2 & 0 & \ldots & I_3 \\ \vdots & & & & \\ 0 & 0 & \ldots & A_1 & 0 \\ 0 & 0 & \ldots & A_2 & I_3 \end{pmatrix} \tag{6}$$

where

$$A_1 = \begin{pmatrix} 1 & 1 \\ 1 & k_{12} \\ 1 & k_{13} \end{pmatrix} \tag{7}$$

and

$$A_2 = \begin{pmatrix} 1 & -1 \\ 1 & -k_{12} \\ 1 & -k_{13} \end{pmatrix} \tag{8}$$

with $K_{12} = (f_1 / f_2)^2$ and $K_{13} = (f_1 / f_3)^2$.

Applying the LS theory, the LS solution we are looking for is given by

$$\begin{pmatrix} \hat{\underline{\xi}}\,(t_1) \\ \hat{\underline{\xi}}\,(t_2) \\ \vdots \\ \hat{\underline{\xi}}\,(tn) \\ \hat{\underline{B}} \end{pmatrix} = (A^+\, Q^{-1}\, A)^{-1}\; A^+\, Q^{-1} \begin{pmatrix} \underline{y}_0\,(t) \\ \underline{y}_0\,(t_2) \\ \vdots \\ \underline{y}_0\;(t_n) \end{pmatrix} = \qquad (9)$$

$$= \begin{pmatrix} A_1^+ Q_P^{-1}\, A_1 + A_2^+\, A_2 & 0 & 0 & \dots & 0 & A_2^+ \\ 0 & A_1^+ Q_P^{-1}\, A_1 + A_2^+\, A_2 & 0 & \dots & 0 & A_2^+ \\ \vdots & \vdots & \ddots & & \vdots & \vdots \\ 0 & 0 & 0 & \dots & A_1^+ Q_P^{-1}\, A_1 + A_2^+\, A_2 & A_2^+ \\ A_2 & A_2 & A_2 & \dots & A_2 & nI_3 \end{pmatrix}^{-1}$$

$$\cdot \begin{pmatrix} A_1^+ Q_P^{-1}\, \underline{P}(t_1) + A_2^+\, \underline{L}(t_1) \\ A_1^+ Q_P^{-1}\, \underline{P}(t_2) + A_2^+\, \underline{L}(t_2) \\ \vdots \\ A_1^+ Q_P^{-1}\, \underline{P}(t_n) + A_2^+\, \underline{L}(t_n) \\ \sum\limits_{t_i} \underline{L}(t_i) \end{pmatrix}$$

where Q is the cofactor matrix.

Now we need to know the expression of the inverse of the normal matrix. We can write

$$N_{-} = \begin{pmatrix} N & 0 & 0 & \dots & 0 & A_2^+ \\ 0 & N & 0 & \dots & 0 & A_2^+ \\ \vdots & \vdots & & & \vdots & \vdots \\ 0 & 0 & 0 & \dots & N & A_2^+ \\ A_2 & A_2 & A_2 & \dots & A_2 & nI_3 \end{pmatrix} \qquad (10)$$

with $N = A_1^+ Q_P^{-1} A_1 + A_2^+ A_2 = M + A_2^+ A_2$; N being a 2 x 2 matrix.

The above matrix can be written as the following block matrix

$$\bar{N} = \begin{pmatrix} \tilde{N} & E \\ E^+ & F \end{pmatrix} \tag{11}$$

where

$$\tilde{N} = \begin{pmatrix} N & 0 & 0 & \dots & 0 \\ 0 & N & 0 & \dots & 0 \\ \vdots & \vdots & & & \\ 0 & 0 & 0 & \dots & N \end{pmatrix} \tag{12}$$

$$E = \begin{pmatrix} A_2^+ \\ A_2^+ \\ \vdots \\ A_2^+ \end{pmatrix} \tag{13}$$

and

$$F = nI_3 \tag{14}$$

where n is equal to the number of epochs.

Taking into account the expression of the inverse of a block matrix (Koch, 1999), we obtain

$$\bar{N}^{-1} = \begin{pmatrix} \Gamma & \Delta \\ \Delta^+ & \gamma \end{pmatrix} \tag{15}$$

where

$$\gamma = \frac{1}{n} (I_3 - A_2 N^{-1} A_2^+)^{-1} \tag{15}$$

$$\Delta = \frac{-1}{n} \begin{pmatrix} N^{-1} A_2^+ D^{-1} \\ N^{-1} A_2^+ D^{-1} \\ \vdots \\ N^{-1} A_2^+ D^{-1} \end{pmatrix} \tag{17}$$

with $D = (I_3 - A_2 N^{-1} A_2^+)$ and

$$\Gamma = N^{-1} \otimes I_n + \frac{1}{n} N^{-1} A_2^+ D^{-1} A_2 N^{-1} \otimes \underline{e} \cdot \underline{e}^+ \tag{18}$$

with $\underline{e} = (1, 1, 1, \ldots, 1)$ and $\otimes$ representing the tensorial product.

It is important to underline that D^{-1} always exists, and, in fact, the inverse matrix of N is

$$N^{-1} = M^{-1} - M^{-1} A_2^+ (I_3 + A_2 M^{-1} A_2^+)^{-1} A_2 M^{-1} \tag{19}$$

Then

$$\begin{aligned} A_2 N^{-1} A_2^+ &= A_2 M^{-1} A_2^+ - A_2 M^{-1} A_2^+ (I_3 + A_2 M^{-1} A_2^+)^{-1} A_2 M^{-1} A_2^+ \\ &= (I_3 + A_2 M^{-1} A_2^+)^{-1} A_2 M^{-1} A_2^+ = I_3 - (I_3 + A_2 M^{-1} A_2^+)^{-1} \end{aligned} \tag{20}$$

Finally, we obtain

$$I_3 - A_2 N^{-1} A_2^+ = (I_3 + A_2 M^{-1} A_2^+)^{-1} \tag{21}$$

The right side of the above equation is always greater than or equal to zero, so we can conclude that the expression of D^{-1} is

$$D^{-1} = (I_3 - A_2 N^{-1} A_2^+)^{-1} = I_3 + A_2 M^{-1} A_2^+ \tag{22}$$

Substituting (16), (17) and (18) in (9), we obtain the expression of the LS solution. In particular, the LS estimation of the ambiguity parameter is given by

$$\begin{aligned} \hat{\underline{B}} &= \frac{-1}{n} \sum_{t_i} D^{-1} A_2 N^{-1} \left(A_1^+ Q_P^{-1} \underline{P}(t_i) + A_2^+ \underline{L}(t_i) \right) + \frac{1}{n} D^{-1} \sum_{t_i} \underline{L}(t_i) \\ &= - D^{-1} A_2 N^{-1} (A_1^+ Q_P^{-1} \bar{\underline{P}} + A_2^+ \bar{\underline{L}}) + D^{-1} \bar{\underline{L}} \\ &= (D^{-1} - D^{-1} A_2 N^{-1} A_2^+) \bar{\underline{L}} - D^{-1} A_2 N^{-1} A_1^+ Q_P^{-1} \bar{\underline{P}} \end{aligned} \tag{23}$$

where $\bar{\underline{P}}$ and $\bar{\underline{L}}$ are the mean of the pseudorange and phase measurements, respectively, over the observation period. The LS solution of the smoothed pseudorange and ionosphere parameters at any epoch t is given by

$$\hat{\underline{\xi}}(t) = \begin{pmatrix} \hat{\underline{\rho}}(t) \\ \hat{\underline{J}}(t) \end{pmatrix}$$

$$\begin{aligned} &= \left(N^{-1} + \frac{1}{n} N^{-1} A_2^+ D^{-1} A_2 N^{-1}\right)\left(A_1^+ Q_P^{-1} \underline{P}(t) + A_2^+ \underline{L}(t)\right) - \frac{1}{n} N^{-1} A_2^+ D^{-1} \sum_{t_i} \underline{L}(t_i) \\ &= \left(N^{-1} + \frac{1}{n} N^{-1} A_2^+ D^{-1} A_2 N^{-1}\right)\left(A_1^+ Q_P^{-1} \underline{P}(t) + A_2^+ \underline{L}(t)\right) - N^{-1} A_2^+ D^{-1} \overline{\underline{L}} \end{aligned} \quad (24)$$

t being the considered epoch and t_i the other epochs of the observation period. Taking the covariance propagation law into account, we obtain the formal covariance matrices of the LS estimates. In this way, the covariance matrix of the ambiguity biases reads

$$C_{\hat{\underline{B}}\hat{\underline{B}}} = \sigma_0^2 \frac{1}{n} (I_3 - A_2 N^{-1} A_2^+)^{-1} \quad (25)$$

and the covariance matrix of the smoothed pseudorange and ionospheric delay parameter at any epoch is

$$C_{\hat{\underline{\zeta}}\hat{\underline{\zeta}}} = \sigma_0^2 (N^{-1} + \frac{1}{n} N^{-1} A_2^+ D^{-1} A_2 N^{-1}) \quad (26)$$

A more elegant way to obtain the LS solution in a dual frequency scenario was presented in (Lacy et al. 2005).

It is important to stress that a subsequent LS estimation is necessary to obtain the receiver position. In particular, the observation vector is formed by the smoothed pseudoranges (24). These smoothed pseudoranges for one receiver and several satellites can be combined to recover the receiver position. The corresponding stochastic model is obtained from (26). This matrix is equal for every pair receiver-satellite and it can be written as

$$C_{\hat{\rho}\hat{\rho}} = \begin{pmatrix} d+a & a & a & \dots & a \\ a & d+a & a & \dots & a \\ \mathrm{a} & \mathrm{a} & \mathrm{d}+\mathrm{a} & \dots & \mathrm{a} \\ a & a & \dots & & d+a \end{pmatrix} = dI_n + a\underline{e}\underline{e}^+ \quad (27)$$

with d, a $d, a \in \mathbb{R}$, I_n the $n \times n$ identity matrix and $\underline{e} = (1, 1, \ldots, 1)^+$. Note that the inverse of this matrix is known and it is given by

$$C_{\hat{\rho}\hat{\rho}}^{-1} = \frac{1}{d}\left(I_n - \frac{a}{d + na}\right)\underline{e}\underline{e}^{+} \tag{28}$$

It is worth remembering that the expression (24) gives the estimation of the ionospheric parameter at any epoch *t*, but it is biased by the term known as equipment delay.

4. NUMERICAL TESTS

Expressions (25) and (26) give explicit expressions of the covariance matrices. We can see that they depend on the observation time. This result allows us to study the theoretical limits for the achievable accuracies. So let us study the behaviour of the standard deviations of the unknowns as a function of time. We will consider the error of the measurements uncorrelated, but we must not forget that the results presented here could be improved with the use of a correlated covariance matrix, especially in pseudoranges. As a consequence of this simplification, the resulting formal accuracies are expected to be optimistic. In order to achieve more realistic results, numerical tests with simulated data were carried out.

The scenarios considered in our study are the following:

1. GPS only, dual and triple frequency.
2. Galileo triple frequency.
3. Galileo simulated data provided by GSSF (Galileo Simulate System Facility), (Zimmermann, 2006).

In the two first scenarios, the noise of the phase measurements is established at 0.002 m. The standard deviations of the code observations are listed in Table 3. In the third case, standard options of the GSSF were used to obtain Galileo triple frequency data.

Under these assumptions, the theoretical standard deviations of the ambiguity biases $(\sigma_{\hat{B}_k})$, smoothed pseudoranges $(\sigma_{\hat{\rho}})$ and ionospheric bias (σ_I) have been studied. In the first scenario, the dual frequency results are based on the current GPS L1 and L2 frequencies and for the triple frequency results the future GPS L5 frequency is added. In Fig. 1 the behaviour of $\sigma_{\hat{B}_k}$ is shown. The same results are

Table 3.- Standard deviation of code observations (meters)

Standard precision			
L1	0.30	E1/E2	0.15
L2	0.30	E5b	0.10
L5	0.10	E5a	0.10

obtained for $\sigma_{\hat{B}_1}$ and $\sigma_{\hat{B}_2}$ in a dual frequency scenario. In a triple frequency hypothesis $\sigma_{\hat{B}_2} = \sigma_{\hat{B}_3}$ and their values are very close to those obtained for the dual frequency scenario. The best results indicate that the standard deviation drops to 0.4 cycles after 200 epochs. These results are not small enough for an unambiguous estimation of $\hat{B}_k$. Therefore, we are looking into the standard deviation of the widelane ambiguities.

Fig. 2 shows the uncertainty of the all possible GPS widelane ambiguity bias (Table 2). Better results are obtained when a third frequency is assumed. The longer the wavelength, the smaller the standard deviation, although the difference between the standard deviation of the mediumlane and widelane ambiguities is very small. For the widelane combination formed by L2 and L5, the standard deviation drops below 0.01 cycles after 10 epochs. It is clear that the new widelane linear combinations will be very useful for detecting and repairing cycle slips. It is important to note that the results relative to a scenario with two GPS frequencies are consistent with those obtained in (Euler and Goad, 1991).

Now, we can study the covariance matrix (26). This matrix can be written as a constant part plus another part which depends on time. Under the above hypothesis, when $n \to +\infty$, only the constant part is left. If we consider a GPS dual frequency scenario, we see that if $n \to +\infty$, $\sigma_{\hat{\rho}} \approx 0.0057$ m and $\sigma_{\hat{I}} \approx 0.0043$ m. If a third GPS frequency is assumed, when $n \to +\infty$, $\sigma_{\hat{\rho}} \approx 0.0051$ m and $\sigma_{\hat{I}} \approx 0.0033$ m. In all cases, if $n \to +\infty$, the formal accuracies

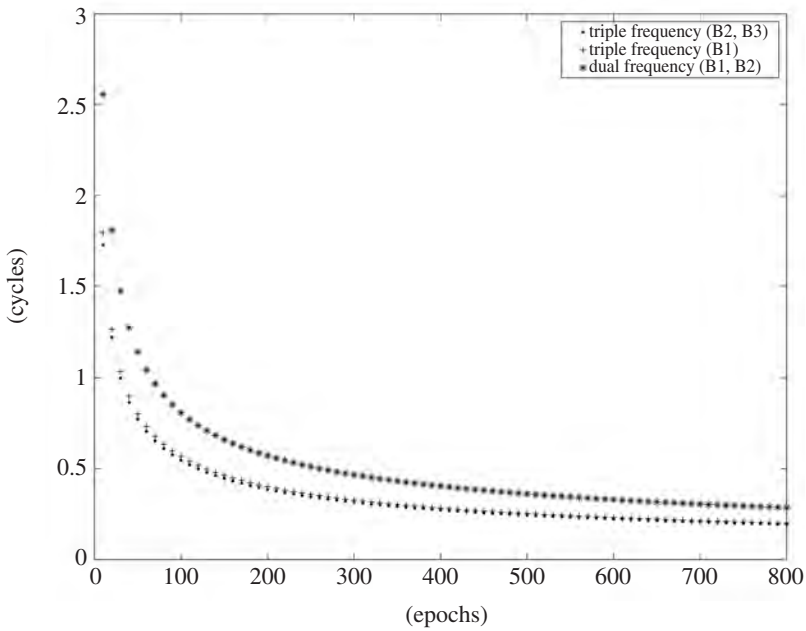

Figure 1.- Standard deviations of ambiguity biases. GPS-only scenario.

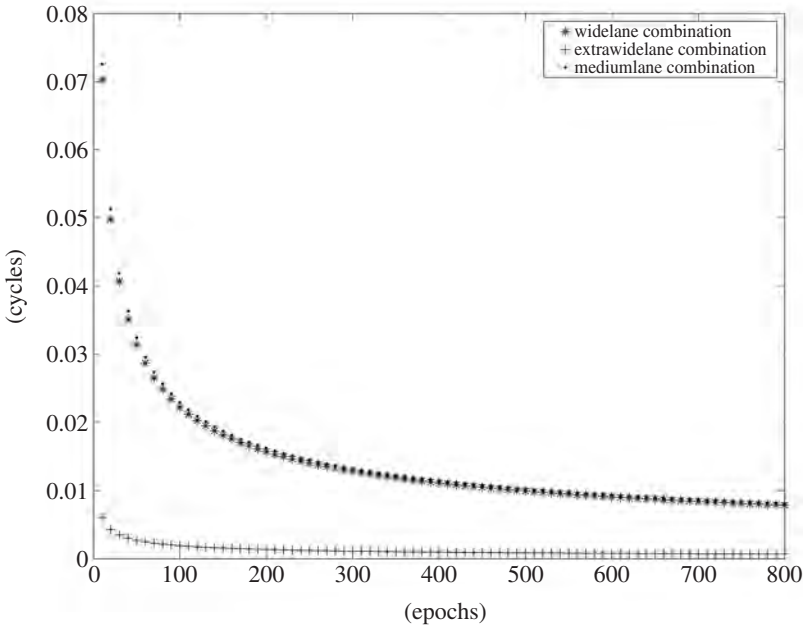

Figure 2.- Standard deviations of widelane ambiguity biases. GPS-only scenario.

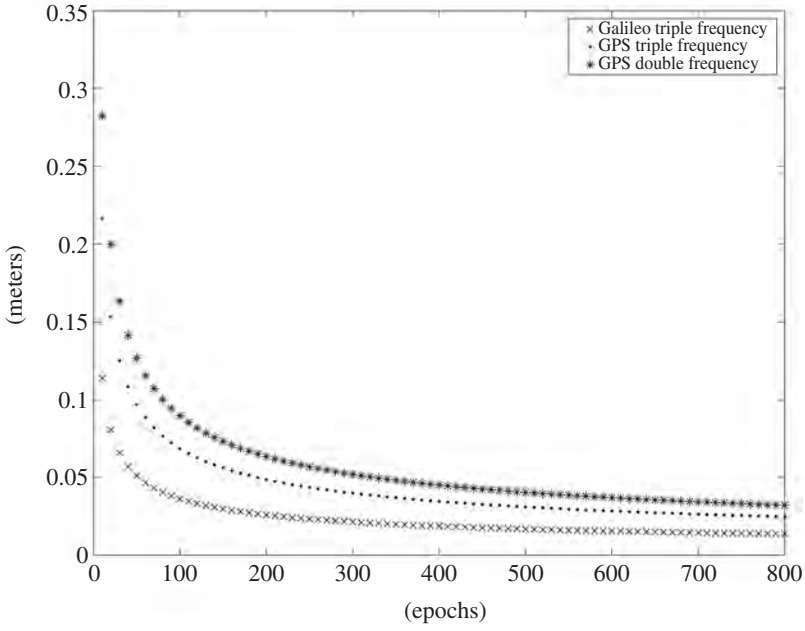

Figure 3.- Standard deviations of smoothed pseudoranges.

are less than 1 cm and no significant differences have been found when a third frequency is introduced. The general behaviour of $\sigma_{\hat{\rho}}$ is shown in Fig. 3. Better results are reached when a third frequency is assumed. In particular, $\sigma_{\hat{\rho}}$ is better than 10 cm after 80 epochs in a dual frequency scenario and $\sigma_{\hat{\rho}}$ is better than 10 cm after 50 epochs in a triple frequency scenario. When the Galileo scenario is considered, the results improve as we will analyze later. In Fig. 4, it can be seen that the formal accuracy of the ionosphere parameter is better than 10 cm after 50 epochs in a dual frequency scenario and after 20 epochs when a third GPS frequency is assumed.

In a Galileo scenario, regarding the standard deviation of the ambiguity biases, the results are very similar to those obtained in a GPS scenario. It is to say that the standard deviation is not small enough for an unambiguous estimation of. The corresponding figures are not included here to avoid a great number of similar figures. Fig. 5 shows the standard deviation of all possible Galileo widelane ambiguity bias (Table 2). Better results are obtained when a third frequency is assumed. As in the GPS scenario, we notice that the longer the wavelength, the smaller the standard deviation. Comparing with GPS-only scenario, we can say that the formal accuracy of Galileo widelane combinations is greater than the relative to GPS widelane combinations. Both, GPS and Galileo widelane combinations will be very useful for detecting and correcting cycle slips. It is important to remember that the LS approach described in Section 3 could also be applied to differenced observations, e. g. single and double

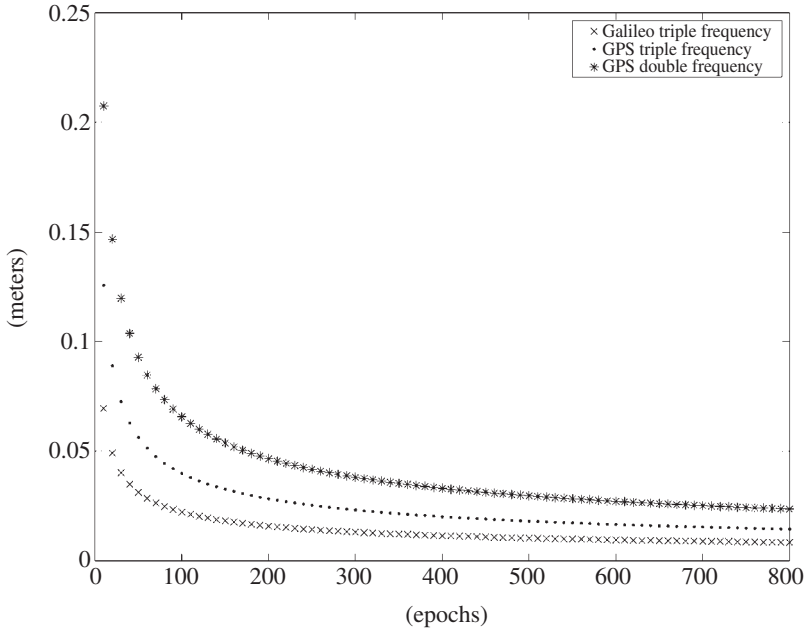

Figure 4.- Standard deviations of ionosphere bias.

difference data. From the above results, it is expected that these new widelane combinations improve and speed up the capability of solving integer ambiguity parameters, mainly by fixing them with a cascading method. It is important to remember that, if we assume an integrated GPS and Galileo scenario, the ambiguities of a mixed pair of double differences are in general not integer, due to different clock characteristics.

Regarding pseudoranges and ionospheric parameters, $\sigma_{\hat{\rho}}$ is close to 10 cm after 10 epochs (Fig. 3) and $\sigma_{\hat{I}}$ is close to 5 cm after 10 epochs (Fig. 4). Comparing Galileo and GPS scenarios, the standard deviation of all parameters considered is, in general, much smaller in the Galileo system.

The results presented here, mainly depend on the standard deviation of the pseudoranges. As there is a discrepancy about these values (Zhang, 2003), (Simsky et al, 2006), Galileo data coming from GSSF with standard options are studied. The Raw Data Generation capability of GSSF is used in order to generate Galileo observations acquired by Galileo Sensor Stations, (Zimmermann, 2006). In our case, the options used to simulate the data set are the following: The total environment delay of the signal from its time of emission to time of reception is calculated by adding free space delay, ionospheric delay and tropospheric delay for each broadcasted frequency. The free space delay simulates the delay due to free space of a signal propagating from a transmitter to a receiver, with eccentricity and "Sagnac" effects, which individually add an offset to ideal free space delay. The ionospheric delay uses

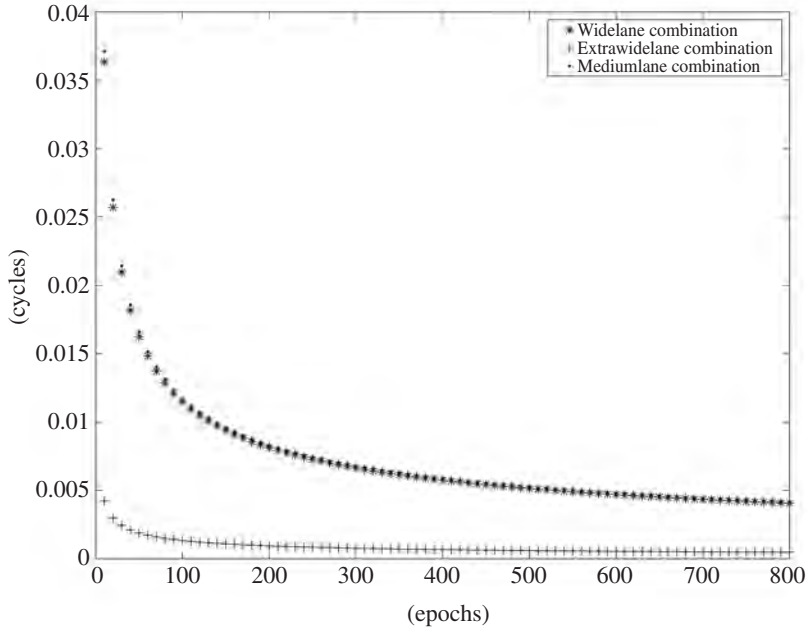

Figure 5.- Standard deviations of widelane ambiguity biases. Galileo scenario.

ITU-R NeQuick to calculate the total electron content (TEC). The TEC, as provided by the ITU-R NeQuick model, is a function of time of day, user location, satellite elevation angle, season and further environmental parameters. The tropospheric model computes tropospheric delay as the sum of dry and wet tropospheric zenith delays, mapped to the satellite elevation angle. The tropospheric delay algorithm is based on the Hopfield model. The Galileo Sensor Station (GSS) is a derivative of the static user receiver model used within GSSF. It consists of a receiver front-end model, which receives the Galileo and GPS signals from the visible satellites and computes the observations to be included into a RINEX file. The pseudorange values are simulated by adding measurement errors to the range (time) information provided by the environment model. These measurement errors are a function of noise, multipath effects and group delay (interfrequency bias). The total signal to noise ratio will be computed from received power, signal propagation noise, intrinsic receiver noise, and interference noise. These options have been used to simulate 1-second Galileo data from 12h to 16h of 7th June 2007 at a point of known coordinates (Fig. 6). Simulated data have been used to check the results obtained from the analysis of the formal accuracy.

From Figs. 7 and 8, the STD obtained from real dual frequency GPS are slightly better than those provided by Galileo simulated data. It is probably linked to the characteristics of GSSF and the high noise of Galileo pseudorange data. In the future, the method will be tested with GIOVE-A data.

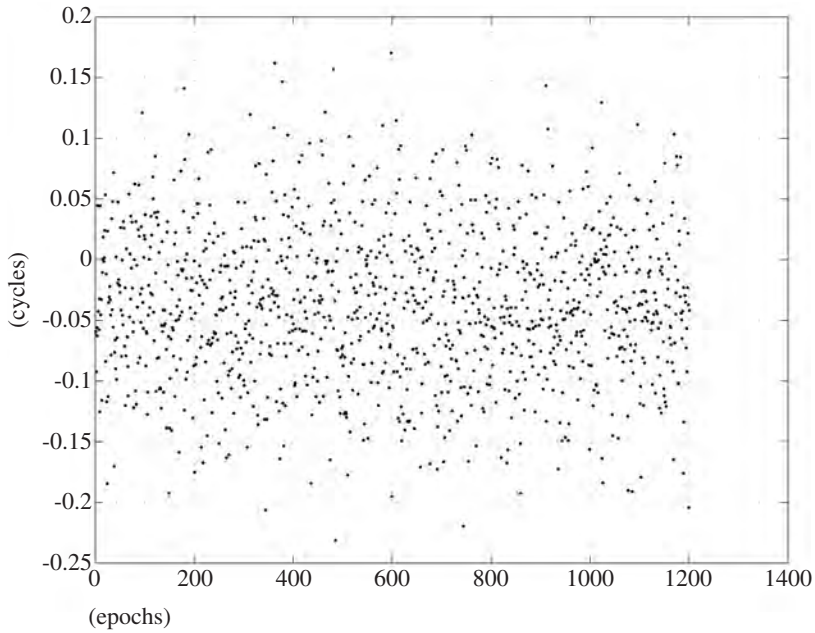

Figure 6.- Galileo simulated data provided by GSSF.

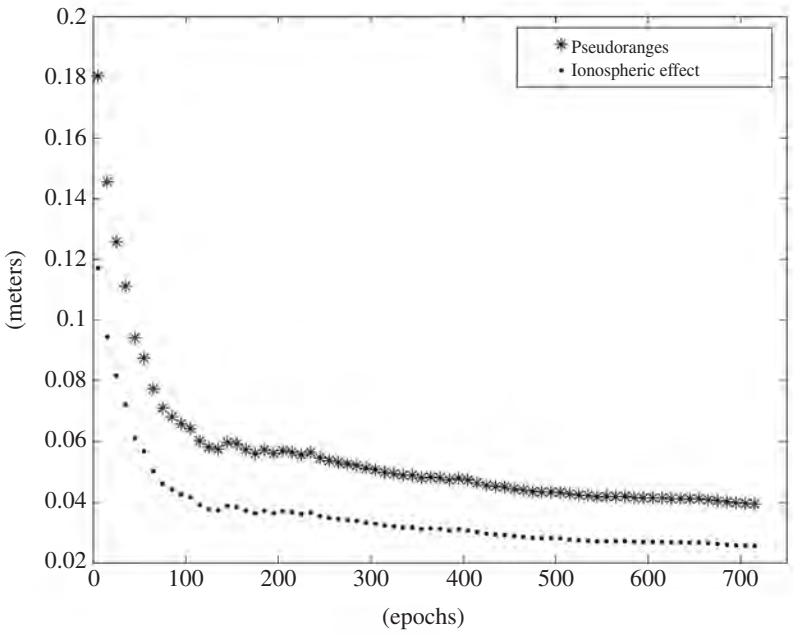

Figure 7.- Standard deviations of smoothed pseudoranges and ionospheric biases. Galileo scenario.

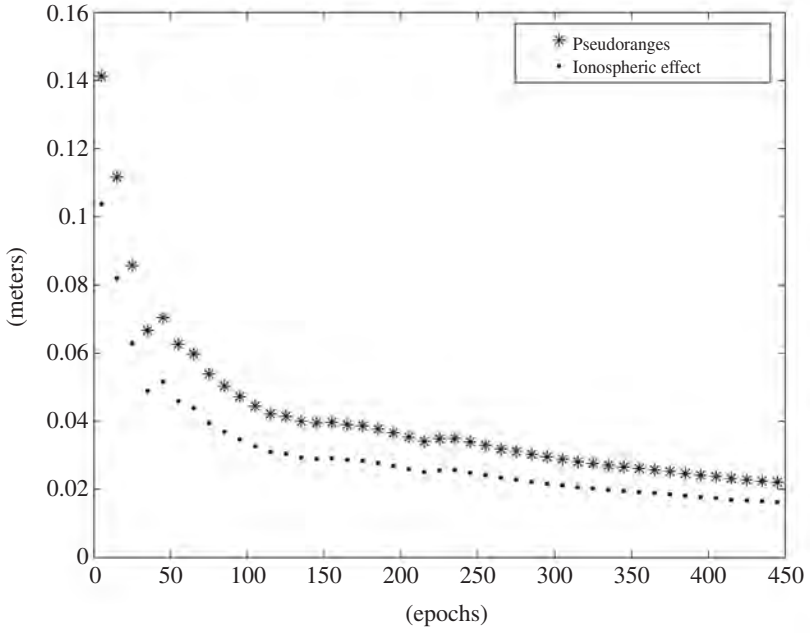

Figure 8.- Standard deviations of pseudoranges and ionospheric bias. Real GPS data.

5. CONCLUSIONS AND FUTURE WORK

In this paper, an LS approach using undifferenced GNSS data to single point positioning is presented. Furthermore, this procedure allows us to estimate the ionospheric bias at any epoch. The covariance matrices of the LS adjustment are explicitly obtained and this has allowed us to study the theoretical limits of the achievable accuracy. The formal accuracies of ambiguity bias, smoothed pseudorange and ionospheric bias are studied under different dual and triple frequency scenarios. The procedure can be used in a multifrequency scenario. In this work, it has been used in different contexts: dual and triple frequency GPS and Galileo systems. This fact has allowed us to analyze the impact of new linear combinations of phase observations. In general, the Galileo solution is better than the GPS one and the results improve when a third frequency is assumed. In particular, the standard deviation of the smoothed pseudoranges is better than 10 cm after 50 epochs in a triple frequency GPS scenario, and is close to 10 cm after 10 epochs in a triple frequency Galileo scenario.

Furthermore, the results stemming from simulated data were compared to the results obtained from real dual frequency. GPS results are slightly better than those provided by Galileo simulated data. It is probably linked to the characteristics of GSSF and the high noise of Galileo pseudorange data. In the future, the method will be tested with GIOVE-A data.

The LS approach presented in this work could be also applied to double differenced observations.

The work presented is framed inside the research Project ESP2005-01997 'Un estudio del impacto de la modernización del GPS y del proyecto europeo Galileo en las técnicas de posicionamiento de precisión' funded by Ministerio de Educación y Ciencia.

6. REFERENCES

BONA P., 2000 Precision, Cross Correlation and Time Correlation of GPS Phase and Code Observations. *GPS Solutions*, 4(2), 3-13.

COCO D.S. COKER C. DAHLKE S.R. & J.R. CLYNCH, 1991. Variability of GPS satellite differential group delay biases. IEEE *Trans. Aerosp. Electron. Syst.*, 7, 931-938.

EULER H. J. & C. C. GOAD, 1991. On optimal filtering of GPS dual frequency observations without using orbit information. *Bulletin Geodesique*, 65, 130-143.

KOCH K. R., 1999. *Parameter Estimation and Hypothesis Testing in Linear Models*. Springer Verlag. Germany.

De LACY M. C. SANSÓ F. GIL A. J. & G. RODRÍGUEZ-CADEROT, 2005. A method for the ionospheric delay estimation and its interpolation in a local GPS network, *Stud. Geophys. Geod.*, 49, 63-84.

PORTILLO A. HERRAIZ M. RADICELLA S.M. & L. CIRAOLO, 2008. Equatorial plasma bubbles studied using African slant total electron content observations. Journal of Atmospheric and Solar-Terrestrial Physics, doi:10.1016/j.jastp.2007.05.019

SARDON E. RIUS A. & N. ZARRAOA, 1994. Estimation of the transmitter and receiver differential biases and the ionospheric total electron content from Global Positioning System observations. *Radio Sci.*, 29, 577-586.

SCHAER S., 1999. Mapping and Prediction the Earth's Ionosphere Using the Global Positioning System. *Geodaetisch-geophysikalische Arbeiten der Schweiz* 59, Swiss Geodetic Commission, Swiiss Academy of Sciences, Bern, Switzerland.

SIMSKY A. SLEEWAEGEN J.M. & P. NEMRY, 2006. Early performance results for new Galileo and GPS signals in space. *Proceedings ENC GNSS, The European Navigation Conference and Exhibition*, Manchester, UK, 8-10 May 2006.

ZHANG W. CANNON M. E. JULIEN O. & P. ALVES, 2003. Investigation of Combined GPS/GALILEO Cascading Ambiguity Resolution Schemes. *ION GPS/GNSS 2003*,Portland, OR, 9-12 September 2003.

ZHANG W., 2005. *Triple Frequency Cascading Ambiguity Resolution for Modernized GPS and Galileo*. Ph.D. Thesis, University of Calgary.

ZIMMERMANN F. HAAK T. & C. HILL, 2006. The Galileo System Simulation Facility-Validation with Real Measurement Data. *Proceedings of ENC06, The European Navigation Conference and Exhibition*, Manchester, UK, 8-10 May 2006.